NASA Technical Memorandum 102652

EQUILIBRIUM RADIATIVE HEATING TABLES FOR EARTH ENTRY

Kenneth Sutton

Lin C. Hartung

May 1990

National Aeronautics and Space Administration

Langley Research Center
Hampton, Virginia 23665

EQUILIBRIUM RADIATIVE HEATING TABLES FOR EARTH ENTRY

Kenneth Sutton
Lin C. Hartung

NASA Langley Research Center
Hampton, VA 23665

Introduction

The recent resurgence of interest in blunt-body atmospheric entry for applications such as aeroassisted orbital transfer and planetary return has engendered a corresponding revival of interest in radiative heating. Radiative heating may be of importance in these blunt-body flows because of the highly energetic shock layer around the blunt nose. Sutton[1] developed an inviscid, stagnation point, radiation-coupled flow-field code for investigating blunt-body atmospheric entry. The method has been compared with ground-based and flight data,[2] and reasonable agreement has been found. To provide information for entry body studies in support of lunar and Mars return scenarios of interest in the 1970's, the code was exercised over a matrix of Earth entry conditions. These results were never published. Recently, this matrix was extended slightly to reflect entry vehicle designs of current interest. The complete results are presented in this report.

Method

The method used is the Radiating, Inviscid Flow, Stagnation Point (RIFSP) code. Details of the method, which is essentially a solution of the radiation-coupled inviscid flow equations at a hemispherical stagnation point, can be found in Sutton.[1] The radiation portion is the equilibrium radiation line group method developed by Nicolet,[3] which includes atomic line and continuum mechanisms, as well as molecular bands.

The RIFSP code was recently updated to FORTRAN V, and its overlay structure was removed in the process. It runs easily on current computers, requiring about 1 second of computer time per iteration on a mainframe and generally about 700 to 5000 iterations per case depending on the magnitude of the radiative flux. Flow fields with very heavy radiation require more iterations. Memory size is no longer a concern for this code with current computers.

Entry Matrix

The matrix of altitude and velocity conditions for which solutions have been obtained was generated by attempting to bracket the flight conditions of most Earth entry bodies and some aeroassist bodies that are currently envisioned. A matrix of these conditions is given in Fig. 1. The range of conditions is limited by the code's ability to solve flows with very heavy radiation. A series of body sizes was also considered at each flight condition to bracket the vehicle designs under consideration. These range from a slender body with a nose radius of 5 cm to a blunt-body with a 10-m nose radius.

Results

The equilibrium radiative heating results obtained for the Earth entry matrix are given in Tables 1-10 for altitudes ranging from 30 to 84 km. For interpolation, the freestream density ρ_∞ (kg/m^3), not the altitude, should be used as the independent variable. The density at each altitude is given in the tables. Each table also includes the entry velocity V in km/s, the nose radius R_n in meters, the radiative heating rate Q_r in MW/m^2, and the shock standoff distance δ in centimeters. The results are plotted in Figures 2-11, showing the variation of the logarithm of radiative heating with the logarithm of the nose radius for various velocities at each altitude (density).

Discussion

The results generally display the expected trends of increasing radiative heating with increasing nose radius or entry velocity. For cases with relatively heavy radiation, an increase in the number of grid points across the shock layer is required to properly resolve the radiation. These cases, at the highest freestream velocities and body nose radii, have been run with 20 grid points instead of the 11 grid points used in all other cases. Using more than 20 grid points causes only a further 1 to 2 percent increase in the radiative heating, and thus does not significantly alter the results. Using more than 11 grid points has a negligible effect (less than 5 percent) at lower velocities and nose radii.

In addition, the high velocity cases (16 and 18 km/s) at the highest altitude (84 km) were run with only five species in the chemistry: N, O, N+, O+, and e-. For the rather extreme conditions of these flow fields, the calculation on the larger species set was found to break down. This is believed to be caused by a breakdown in the chemistry curve fits at the very high temperatures encountered in these flow fields. The curve fits were generated for temperatures of at most 10000 K, whereas temperatures in these flow fields are of the order of 12000 K, and densities are very low. The combination of these two extremes is believed to be beyond the capacity of the chemistry solution as it exists. However, based on a radiationless solution for these cases, the largest mole fraction of the ignored species is $6x\,10^{-7}$. Therefore, ignoring these species should have a negligible effect.

Note that this is strictly an equilibrium method. Nonequilibrium effects, which may be important particularly for the higher altitude cases, have been completely ignored. Also, since the method is for inviscid flows, the influence of the viscous boundary layer, which might be expected to absorb some fraction of the radiation, has been neglected.

Conclusion

A matrix of equilibrium radiative heating results has been generated for Earth entry. These results have been presented in tabular and graphical form for use in design and parametric studies.

References

1. Sutton, Kenneth, "Characteristics of Coupled Nongray Radiating Gas Flows with Ablation Products Effects About Blunt Bodies During Planetary Entries," PhD Thesis, North Carolina State University, Raleigh, North Carolina, 1973.

2. Sutton, Kenneth, "Air Radiation Revisited," in *Progress in Astronautics and Aeronautics: Thermal Design of Aeroassisted Orbital Transfer Vehicles*, ed. H.F. Nelson, vol. 96, pp. 419-441, AIAA, New York, 1985.

3. Nicolet, W. E., "Advanced Methods for Calculating Radiation Transport in Ablation-Product Contaminated Boundary Layers," NASA CR-1656, Sept. 1970.

Table 1. Radiative Heating Prediction at 30 km Altitude. ($\rho_\infty = 1.8410E-2\ kg/m^3$)

V, km/s	R_n, m	Q_r, MW/m^2	δ, cm
8.0	0.05	1.332	2.655E-01
	0.10	2.410	5.310E-01
	0.23	4.884	1.221
	0.50	9.482	2.655
	1.00	1.664E+01	5.290
	2.30	3.074E+01	1.210E+01
	5.00	5.155E+01	2.610E+01
	10.00	7.685E+01	5.150E+01
8.5	0.05	2.208	2.620E-01
	0.10	3.815	5.240E-01
	0.23	7.609	1.205
	0.50	1.460E+01	2.620
	1.00	2.531E+01	5.220
	2.30	4.682E+01	1.189E+01
	5.00	7.750E+01	2.560E+01
	10.00	1.123E+02	5.040E+01
9.0	0.05	4.006	2.625E-01
	0.10	6.676	5.250E-01
	0.23	1.283E+01	1.205
	0.50	2.389E+01	2.610
	1.00	4.093E+01	5.190
	2.30	7.386E+01	1.180E+01
	5.00	1.184E+02	2.525E+01
	10.00	1.649E+02	4.950E+01
9.5	0.05	9.316	2.675E-01
	0.10	1.442E+01	5.350E-01
	0.23	2.578E+01	1.224
	0.50	4.517E+01	2.645
	1.00	7.376E+01	5.240
	2.30	1.259E+02	1.184E+01
	5.00	1.911E+02	2.515E+01
	10.00	2.514E+02	4.910E+01

V, km/s	R_n, m	Q_r, MW/m^2	δ, cm
10.0	0.05	2.668E+01	2.740E-01
	0.10	3.868E+01	5.460E-01
	0.23	6.305E+01	1.247
	0.50	1.011E+02	2.675
	1.00	1.508E+02	5.270
	2.30	2.325E+02	1.180E+01
	5.00	3.201E+02	2.490E+01
	10.00	3.861E+02	4.830E+01
11.0	0.05	1.269E+02	2.765E-01
	0.10	1.703E+02	5.480E-01
	0.23	2.468E+02	1.240
	0.50	3.460E+02	2.635
	1.00	4.550E+02	5.140
	2.30	5.962E+02	1.138E+01
	5.00	7.013E+02	2.385E+01
	10.00	7.709E+02	4.590E+01
12.0	0.05	3.097E+02	2.700E-01
	0.10	3.961E+02	5.330E-01
	0.23	5.421E+02	1.196
	0.50	7.171E+02	2.525
	1.00	8.923E+02	4.890
	2.30	1.077E+03	1.079E+01
	5.00	1.215E+03	2.230E+01
	10.00	1.171E+03	4.360E+01

Table 2. Radiative Heating Prediction at 36 km Altitude. ($\rho_\infty = 7.2579E{-}3\ kg/m^3$)

V, km/s	R_n, m	Q_r, MW/m^2	δ, cm
8.0	0.05	2.493E-01	2.550E-01
	0.10	4.548E-01	5.100E-01
	0.23	9.506E-01	1.173
	0.50	1.871	2.550
	1.00	3.482	5.100
	2.30	7.120	1.168E+01
	5.00	1.317E+01	2.525E+01
	10.00	2.194E+01	4.990E+01
8.5	0.05	4.345E-01	2.520E-01
	0.10	7.658E-01	5.040E-01
	0.23	1.517	1.159
	0.50	2.931	2.520
	1.00	5.358	5.030
	2.30	1.084E+01	1.152E+01
	5.00	1.994E+01	2.485E+01
	10.00	3.286E+01	4.900E+01
9.0	0.05	9.116E-01	2.530E-01
	0.10	1.476	5.060E-01
	0.23	2.711	1.164
	0.50	5.032	2.525
	1.00	8.889	5.040
	2.30	1.749E+01	1.150E+01
	5.00	3.151E+01	2.470E+01
	10.00	5.016E+01	4.850E+01
9.5	0.05	2.659	2.600E-01
	0.10	3.963	5.190E-01
	0.23	6.640	1.191
	0.50	1.115E+01	2.580
	1.00	1.824E+01	5.130
	2.30	3.312E+01	1.166E+01
	5.00	5.572E+01	2.480E+01
	10.00	8.326E+01	4.820E+01
10.0	0.05	9.384	2.670E-01
	0.10	1.296E+01	5.330E-01
	0.23	1.963E+01	1.219
	0.50	3.010E+01	2.625
	1.00	4.492E+01	5.190
	2.30	7.213E+01	1.168E+01
	5.00	1.082E+02	2.460E+01
	10.00	1.470E+02	4.750E+01
11.0	0.05	4.716E+01	2.680E-01
	0.10	6.065E+01	5.320E-01
	0.23	8.480E+01	1.207
	0.50	1.188E+02	2.575
	1.00	1.604E+02	5.030
	2.30	2.232E+02	1.115E+01
	5.00	2.887E+02	2.315E+01
	10.00	3.574E+02	4.370E+01
12.0	0.05	1.178E+02	2.605E-01
	0.10	1.459E+02	5.150E-01
	0.23	1.951E+02	1.159
	0.50	2.611E+02	2.450
	1.00	3.361E+02	4.720
	2.30	4.368E+02	1.042E+01
	5.00	5.264E+02	2.150E+01
	10.00	6.196E+02	4.020E+01
14.0	0.05	3.569E+02	2.435E-01
	0.10	4.168E+02	4.770E-01
	0.23	5.242E+02	1.060
	0.50	6.666E+02	2.210
	1.00	8.209E+02	4.230
	2.30	1.001E+03	9.108
	5.00	1.189E+03	1.820E+01
	10.00	1.234E+03	3.480E+01

Table 3. Radiative Heating Prediction at 42 km Altitude. ($\rho_\infty = 2.9948E-3\ kg/m^3$)

V, km/s	R_n, m	Q_r, MW/m^2	δ, cm
8.0	0.05	5.083E-02	2.455E-01
	0.10	9.289E-02	4.910E-01
	0.23	1.946E-01	1.129
	0.50	3.918E-01	2.455
	1.00	7.251E-01	4.910
	2.30	1.550	1.129E+01
	5.00	3.090	2.450E+01
	10.00	5.603	4.850E+01
8.5	0.05	9.308E-02	2.430E-01
	0.10	1.633E-01	4.860E-01
	0.23	3.268E-01	1.118
	0.50	6.296E-01	2.430
	1.00	1.136	4.860
	2.30	2.380	1.113E+01
	5.00	4.701	2.410E+01
	10.00	8.361	4.780E+01
9.0	0.05	2.124E-01	2.450E-01
	0.10	3.515E-01	4.900E-01
	0.23	6.467E-01	1.125
	0.50	1.153	2.445
	1.00	2.008	4.890
	2.30	4.008	1.120E+01
	5.00	7.657	2.415E+01
	10.00	1.313E+01	4.770E+01
9.5	0.05	8.145E-01	2.535E-01
	0.10	1.231	5.060E-01
	0.23	2.002	1.164
	0.50	3.212	2.525
	1.00	5.012	5.020
	2.30	8.851	1.145E+01
	5.00	1.528E+01	2.450E+01
	10.00	2.415E+01	4.790E+01

V, km/s	R_n, m	Q_r, MW/m^2	δ, cm
10.0	0.05	3.336	2.610E-01
	0.10	4.720	5.200E-01
	0.23	7.026	1.191
	0.50	1.018E+01	2.570
	1.00	1.446E+01	5.100
	2.30	2.266E+01	1.152E+01
	5.00	3.471E+01	2.450E+01
	10.00	4.914E+01	4.740E+01
11.0	0.05	1.767E+01	2.600E-01
	0.10	2.315E+01	5.160E-01
	0.23	3.135E+01	1.175
	0.50	4.201E+01	2.520
	1.00	5.557E+01	4.940
	2.30	7.849E+01	1.102E+01
	5.00	1.056E+02	2.300E+01
	10.00	1.316E+02	4.400E+01
12.0	0.05	4.535E+01	2.525E-01
	0.10	5.667E+01	4.990E-01
	0.23	7.286E+01	1.127
	0.50	9.429E+01	2.395
	1.00	1.208E+02	4.660
	2.30	1.618E+02	1.026E+01
	5.00	2.047E+02	2.120E+01
	10.00	2.553E+02	3.950E+01
14.0	0.05	1.437E+02	2.355E-01
	0.10	1.689E+02	4.600E-01
	0.23	2.044E+02	1.028
	0.50	2.518E+02	2.150
	1.00	3.090E+02	4.120
	2.30	4.105E+02	8.740
	5.00	4.945E+02	1.765E+01
	10.00	5.560E+02	3.330E+01

Table 4. Radiative Heating Prediction at 48 km Altitude. ($\rho_\infty = 1.3167E-3\ kg/m^3$)

V, km/s	R_n, m	Q_r, MW/m^2	δ, cm
9.0	0.05	5.477E-02	2.380E-01
	0.10	9.356E-02	4.750E-01
	0.23	1.741E-01	1.093
	0.50	3.077E-01	2.375
	1.00	5.193E-01	4.750
	2.30	1.012	1.090E+01
	5.00	1.936	2.360E+01
	10.00	3.435	4.660E+01
9.5	0.05	2.660E-01	2.480E-01
	0.10	4.080E-01	4.960E-01
	0.23	6.803E-01	1.139
	0.50	1.084	2.470
	1.00	1.644	4.930
	2.30	2.758	1.127E+01
	5.00	4.588	2.425E+01
	10.00	7.275	4.770E+01
10.0	0.05	1.174	2.550E-01
	0.10	1.734	5.080E-01
	0.23	2.674	1.166
	0.50	3.882	2.520
	1.00	5.377	5.010
	2.30	8.017	1.207E+01
	5.00	1.185E+01	2.425E+01
	10.00	1.688E+01	4.740E+01
11.0	0.05	6.404	2.535E-01
	0.10	8.824	5.030E-01
	0.23	1.239E+01	1.145
	0.50	1.650E+01	2.460
	1.00	2.119E+01	4.840
	2.30	2.897E+01	1.088E+01
	5.00	3.905E+01	2.290E+01
	10.00	4.996E+01	4.400E+01
12.0	0.05	1.684E+01	2.455E-01
	0.10	2.227E+01	4.860E-01
	0.23	2.958E+01	1.099
	0.50	3.745E+01	2.340
	1.00	4.639E+01	4.580
	2.30	6.098E+01	1.017E+01
	5.00	7.856E+01	2.115E+01
	10.00	1.015E+02	3.950E+01
14.0	0.05	5.597E+01	2.300E-01
	0.10	7.013E+01	4.490E-01
	0.23	8.603E+01	1.003
	0.50	1.025E+02	2.110
	1.00	1.278E+02	4.010
	2.30	1.617E+02	8.671
	5.00	1.992E+02	1.755E+01
	10.00	2.324E+02	3.280E+01
16.0	0.05	1.229E+02	2.175E-01
	0.10	1.486E+02	4.190E-01
	0.23	1.726E+02	9.223E-01
	0.50	1.960E+02	1.915
	1.00	2.400E+02	3.570
	2.30	2.953E+02	7.544
	5.00	3.522E+02	1.505E+01
	10.00	3.973E+02	2.760E+01

Table 5. Radiative Heating Prediction at 54 km Altitude. ($\rho_\infty = 6.3137E{-}4\ kg/m^3$)

V, km/s	R_n, m	Q_r, MW/m^2	δ, cm
9.0	0.05	1.526E-02	2.325E-01
	0.10	2.710E-02	4.650E-01
	0.23	5.316E-02	1.067
	0.50	9.716E-02	2.320
	1.00	1.632E-01	4.640
	2.30	3.062E-01	1.065E+01
	5.00	5.744E-01	2.310E+01
	10.00	1.021	4.590E+01
9.5	0.05	9.657E-02	2.435E-01
	0.10	1.521E-01	4.870E-01
	0.23	2.582E-01	1.118
	0.50	4.147E-01	2.425
	1.00	6.268E-01	4.840
	2.30	1.029	1.109E+01
	5.00	1.651	2.390E+01
	10.00	2.549	4.730E+01
10.0	0.05	4.329E-01	2.495E-01
	0.10	6.610E-01	4.980E-01
	0.23	1.064	1.143
	0.50	1.598	2.470
	1.00	2.239	4.910
	2.30	3.293	1.118E+01
	5.00	4.707	2.400E+01
	10.00	6.547	4.720E+01
11.0	0.05	2.355	2.475E-01
	0.10	3.438	4.920E-01
	0.23	5.090	1.122
	0.50	7.006	2.410
	1.00	9.059	4.760
	2.30	1.215E+01	1.072E+01
	5.00	1.598E+01	2.270E+01
	10.00	2.045E+01	4.410E+01

V, km/s	R_n, m	Q_r, MW/m^2	δ, cm
12.0	0.05	6.297	2.400E-01
	0.10	8.886	4.750E-01
	0.23	1.250E+01	1.074
	0.50	1.635E+01	2.295
	1.00	2.024E+01	4.500
	2.30	2.592E+01	1.003E+01
	5.00	3.270E+01	2.105E+01
	10.00	4.253E+01	3.970E+01
14.0	0.05	2.148E+01	2.255E-01
	0.10	2.923E+01	4.410E-01
	0.23	3.839E+01	9.844E-01
	0.50	4.669E+01	2.070
	1.00	5.447E+01	4.010
	2.30	6.961E+01	8.625
	5.00	8.532E+01	1.760E+01
	10.00	1.015E+02	3.290E+01
16.0	0.05	4.784E+01	2.155E-01
	0.10	6.393E+01	4.150E-01
	0.23	8.004E+01	9.085E-01
	0.50	9.217E+01	1.885
	1.00	1.083E+02	3.540
	2.30	1.291E+02	7.567
	5.00	1.541E+02	1.515E+01
	10.00	1.774E+02	2.790E+01
18.0	0.05	8.421E+01	2.115E-01
	0.10	1.127E+02	4.000E-01
	0.23	1.370E+02	8.556E-01
	0.50	1.509E+02	1.740
	1.00	1.646E+02	3.250
	2.30	2.000E+02	6.670
	5.00	2.344E+02	1.310E+01
	10.00	2.575E+02	2.420E+01

Table 6. Radiative Heating Prediction at 60 km Altitude. ($\rho_\infty = 3.0592E-4\ kg/m^3$)

V, km/s	R_n, m	Q_r, MW/m^2	δ, cm
9.0	0.05	4.066E-03	2.275E-01
	0.10	7.402E-03	4.550E-01
	0.23	1.518E-02	1.046
	0.50	2.926E-02	2.270
	1.00	5.156E-02	4.540
	2.30	9.884E-02	1.042E+01
	5.00	1.822E-01	2.265E+01
	10.00	3.223E-01	4.500E+01
9.5	0.05	3.462E-02	2.395E-01
	0.10	5.639E-02	4.790E-01
	0.23	9.802E-02	1.099
	0.50	1.618E-01	2.385
	1.00	2.470E-01	4.770
	2.30	4.021E-01	1.092E+01
	5.00	6.324E-01	2.360E+01
	10.00	9.508E-01	4.680E+01
10.0	0.05	1.539E-01	2.445E-01
	0.10	2.391E-01	4.880E-01
	0.23	4.020E-01	1.120
	0.50	6.277E-01	2.425
	1.00	9.077E-01	4.830
	2.30	1.360	1.102E+01
	5.00	1.940	2.365E+01
	10.00	2.644	4.660E+01
11.0	0.05	8.078E-01	2.415E-01
	0.10	1.246	4.810E-01
	0.23	1.974	1.097
	0.50	2.860	2.360
	1.00	3.822	4.670
	2.30	5.196	1.056E+01
	5.00	6.784	2.250E+01
	10.00	8.543	4.370E+01

V, km/s	R_n, m	Q_r, MW/m^2	δ, cm
12.0	0.05	2.174	2.345E-01
	0.10	3.281	4.650E-01
	0.23	4.996	1.053
	0.50	6.872	2.250
	1.00	8.765	4.430
	2.30	1.130E+01	9.913
	5.00	1.411E+01	2.085E+01
	10.00	1.701E+01	4.010E+01
14.0	0.05	7.540	2.215E-01
	0.10	1.112E+01	4.340E-01
	0.23	1.607E+01	9.706E-01
	0.50	2.065E+01	2.040
	1.00	2.472E+01	3.960
	2.30	2.969E+01	8.694
	5.00	3.720E+01	1.765E+01
	10.00	4.383E+01	3.330E+01
16.0	0.05	1.688E+01	2.135E-01
	0.10	2.480E+01	4.130E-01
	0.23	3.478E+01	9.039E-01
	0.50	4.258E+01	1.870
	1.00	4.854E+01	3.570
	2.30	5.510E+01	7.774
	5.00	6.810E+01	1.525E+01
	10.00	7.830E+01	2.830E+01
18.0	0.05	2.924E+01	2.130E-01
	0.10	4.355E+01	4.040E-01
	0.23	6.087E+01	8.625E-01
	0.50	7.203E+01	1.740
	1.00	7.927E+01	3.250
	2.30	9.170E+01	6.693
	5.00	1.045E+02	1.325E+01
	10.00	1.174E+02	2.430E+01

Table 7. Radiative Heating Prediction at 66 km Altitude. ($\rho_\infty = 1.4713E{-}4\ kg/m^3$)

V, km/s	R_n, m	Q_r, MW/m^2	δ, cm
9.0	0.05	1.066E-03	2.225E-01
	0.10	1.954E-03	4.450E-01
	0.23	4.083E-03	1.023
	0.50	8.107E-03	2.225
	1.00	1.484E-02	4.440
	2.30	3.010E-02	1.021E+01
	5.00	5.611E-02	2.215E+01
	10.00	9.815E-02	4.430E+01
9.5	0.05	1.192E-02	2.350E-01
	0.10	1.980E-02	4.700E-01
	0.23	3.567E-02	1.081
	0.50	6.070E-02	2.345
	1.00	9.651E-02	4.690
	2.30	1.612E-01	1.074E+01
	5.00	2.503E-01	2.325E+01
	10.00	3.696E-01	4.620E+01
10.0	0.05	5.211E-02	2.390E-01
	0.10	8.288E-02	4.780E-01
	0.23	1.442E-01	1.097
	0.50	2.347E-01	2.380
	1.00	3.497E-01	4.740
	2.30	5.428E-01	1.081E+01
	5.00	7.805E-01	2.325E+01
	10.00	1.069	4.600E+01
11.0	0.05	2.591E-01	2.355E-01
	0.10	4.116E-01	4.700E-01
	0.23	6.968E-01	1.074
	0.50	1.074	2.315
	1.00	1.511	4.590
	2.30	2.148	1.037E+01
	5.00	2.845	2.215E+01
	10.00	3.590	4.320E+01

V, km/s	R_n, m	Q_r, MW/m^2	δ, cm
12.0	0.05	6.892E-01	2.285E-01
	0.10	1.089	4.550E-01
	0.23	1.800	1.035
	0.50	2.672	2.215
	1.00	3.585	4.360
	2.30	4.810	9.775
	5.00	6.056	2.065E+01
	10.00	7.340	4.000E+01
14.0	0.05	2.405	2.170E-01
	0.10	3.773	4.280E-01
	0.23	6.020	9.591E-01
	0.50	8.454	2.020
	1.00	1.065E+01	3.920
	2.30	1.323E+01	8.648
	5.00	1.560E+01	1.800E+01
	10.00	1.907E+01	3.360E+01
16.0	0.05	5.401	2.105E-01
	0.10	8.473	4.110E-01
	0.23	1.335E+01	9.062E-01
	0.50	1.814E+01	1.870
	1.00	2.181E+01	3.570
	2.30	2.559E+01	7.728
	5.00	3.050E+01	1.540E+01
	10.00	3.470E+01	2.870E+01
18.0	0.05	9.138	2.135E-01
	0.10	1.465E+01	4.100E-01
	0.23	2.343E+01	8.809E-01
	0.50	3.145E+01	1.775
	1.00	3.667E+01	3.300
	2.30	4.125E+01	6.946
	5.00	4.760E+01	1.350E+01
	10.00	5.260E+01	2.460E+01

Table 8. Radiative Heating Prediction at 72 km Altitude. ($\rho_\infty = 6.6593E-5\ kg/m^3$)

V, km/s	R_n, m	Q_r, MW/m^2	δ, cm
9.0	0.05	2.619E-04	2.180E-01
	0.10	4.789E-04	4.360E-01
	0.23	1.004E-03	1.003
	0.50	2.016E-03	2.180
	1.00	3.759E-03	4.360
	2.30	7.889E-03	1.003E+01
	5.00	1.550E-02	2.175E+01
	10.00	2.731E-02	4.340E+01
9.5	0.05	3.420E-03	2.305E-01
	0.10	5.749E-03	4.610E-01
	0.23	1.076E-02	1.060
	0.50	1.891E-02	2.300
	1.00	3.176E-02	4.600
	2.30	5.744E-02	1.056E+01
	5.00	9.484E-02	2.285E+01
	10.00	1.424E-01	4.540E+01
10.0	0.05	1.576E-02	2.330E-01
	0.10	2.512E-02	4.660E-01
	0.23	4.497E-02	1.072
	0.50	7.685E-02	2.325
	1.00	1.207E-01	4.630
	2.30	1.965E-01	1.060E+01
	5.00	2.939E-01	2.285E+01
	10.00	4.052E-01	4.530E+01
11.0	0.05	7.573E-02	2.290E-01
	0.10	1.204E-01	4.580E-01
	0.23	2.109E-01	1.049
	0.50	3.463E-01	2.260
	1.00	5.131E-01	4.490
	2.30	7.794E-01	1.019E+01
	5.00	1.082	2.180E+01
	10.00	1.389	4.270E+01

V, km/s	R_n, m	Q_r, MW/m^2	δ, cm
12.0	0.05	1.995E-01	2.220E-01
	0.10	3.145E-01	4.430E-01
	0.23	5.414E-01	1.010
	0.50	8.674E-01	2.175
	1.00	1.252	4.290
	2.30	1.804	9.637
	5.00	2.382	2.040E+01
	10.00	2.918	3.960E+01
14.0	0.05	6.750E-01	2.115E-01
	0.10	1.079	4.190E-01
	0.23	1.847	9.476E-01
	0.50	2.867	2.005
	1.00	3.947	3.900
	2.30	5.270	8.602
	5.00	6.465	1.790E+01
	10.00	7.443	3.410E+01
16.0	0.05	1.491	2.065E-01
	0.10	2.418	4.060E-01
	0.23	4.146	9.039E-01
	0.50	6.342	1.885
	1.00	8.453	3.600
	2.30	1.066E+01	7.751
	5.00	1.239E+01	1.590E+01
	10.00	1.452E+01	2.920E+01
18.0	0.05	2.501	2.110E-01
	0.10	4.074	4.110E-01
	0.23	7.169	8.993E-01
	0.50	1.107E+01	1.830
	1.00	1.459E+01	3.400
	2.30	1.773E+01	7.130
	5.00	2.048E+01	1.415E+01
	10.00	2.234E+01	2.560E+01

Table 9. Radiative Heating Prediction at 78 km Altitude. ($\rho_\infty = 2.5239E-5\ kg/m^3$)

V, km/s	R_n, m	Q_r, MW/m^2	δ, cm
9.0	0.05	4.728E-05	2.130E-01
	0.10	8.719E-05	4.260E-01
	0.23	1.833E-04	9.820E-01
	0.50	3.698E-04	2.130
	1.00	6.922E-04	4.260
	2.30	1.476E-03	9.798
	5.00	2.983E-03	2.125E+01
	10.00	5.630E-03	4.250E+01
9.5	0.05	6.853E-04	2.250E-01
	0.10	1.154E-03	4.500E-01
	0.23	2.193E-03	1.033
	0.50	4.055E-03	2.245
	1.00	6.975E-03	4.480
	2.30	1.317E-02	1.033E+01
	5.00	2.356E-02	2.240E+01
	10.00	3.891E-02	4.460E+01
10.0	0.05	3.168E-03	2.265E-01
	0.10	5.248E-03	4.530E-01
	0.23	9.373E-03	1.040
	0.50	1.667E-02	2.260
	1.00	2.793E-02	4.510
	2.30	5.058E-02	1.033E+01
	5.00	8.350E-02	2.230E+01
	10.00	1.251E-01	4.430E+01
11.0	0.05	1.640E-02	2.215E-01
	0.10	2.590E-02	4.420E-01
	0.23	4.585E-02	1.012
	0.50	7.863E-02	2.195
	1.00	1.250E-01	4.370
	2.30	2.068E-01	9.959
	5.00	3.096E-01	2.140E+01
	10.00	4.250E-01	4.190E+01

V, km/s	R_n, m	Q_r, MW/m^2	δ, cm
12.0	0.05	4.333E-02	2.140E-01
	0.10	6.752E-02	4.280E-01
	0.23	1.168E-01	9.798E-01
	0.50	1.951E-01	2.110
	1.00	3.027E-01	4.190
	2.30	4.817E-01	9.453
	5.00	6.938E-01	2.015E+01
	10.00	9.172E-01	3.930E+01
14.0	0.05	1.435E-01	2.035E-01
	0.10	2.247E-01	4.060E-01
	0.23	3.873E-01	9.223E-01
	0.50	6.393E-01	1.975
	1.00	9.707E-01	3.870
	2.30	1.478	8.579
	5.00	2.009	1.790E+01
	10.00	2.493	3.430E+01
16.0	0.05	3.153E-01	1.990E-01
	0.10	4.969E-01	3.950E-01
	0.23	8.626E-01	8.924E-01
	0.50	1.419	1.890
	1.00	2.120	3.650
	2.30	3.245	7.889
	5.00	4.141	1.610E+01
	10.00	4.840	3.030E+01
18.0	0.05	.5798	.2055
	0.10	.9102	.404
	0.23	1.529	.9039
	0.50	2.558	1.880
	1.00	3.773	3.550
	2.30	5.593	7.406
	5.00	6.986	1.465E+01
	10.00	7.984	2.660E+01

Table 10. Radiative Heating Prediction at 84 km Altitude. ($\rho_\infty = 9.6940E-6\ kg/m^3$)

V, km/s	R_n, m	Q_r, MW/m^2	δ, cm
9.0	0.05	9.285E-06	2.090E-01
	0.10	1.749E-05	4.180E-01
	0.23	3.748E-05	9.614E-01
	0.50	7.665E-05	2.090
	1.00	1.455E-04	4.180
	2.30	3.138E-04	9.614
	5.00	6.390E-04	2.090E+01
	10.00	1.199E-03	4.170E+01
9.5	0.05	1.423E-04	2.195E-01
	0.10	2.442E-04	4.390E-01
	0.23	4.653E-04	1.010
	0.50	8.583E-04	2.190
	1.00	1.497E-03	4.380
	2.30	2.927E-03	1.007E+01
	5.00	5.296E-03	2.180E+01
	10.00	8.960E-03	4.350E+01
10.0	0.05	6.142E-04	2.195E-01
	0.10	1.032E-03	4.390E-01
	0.23	1.929E-03	1.010
	0.50	3.406E-03	2.195
	1.00	5.746E-03	4.390
	2.30	1.090E-02	1.007E+01
	5.00	1.945E-02	2.180E+01
	10.00	3.146E-02	4.340E+01
11.0	0.05	3.181E-03	2.135E-01
	0.10	5.120E-03	4.270E-01
	0.23	9.155E-03	9.821E-01
	0.50	1.611E-02	2.130
	1.00	2.704E-02	4.250
	2.30	4.958E-02	9.706
	5.00	8.296E-02	2.090E+01
	10.00	1.233E-01	4.130E+01

V, km/s	R_n, m	Q_r, MW/m^2	δ, cm
12.0	0.05	8.620E-03	2.065E-01
	0.10	1.385E-02	4.130E-01
	0.23	2.462E-02	9.476E-01
	0.50	4.281E-02	2.055
	1.00	7.001E-02	4.080
	2.30	1.230E-01	9.269
	5.00	1.943E-01	2.075E+01
	10.00	2.724E-01	3.870E+01
14.0	0.05	3.181E-02	1.965E-01
	0.10	5.057E-02	3.910E-01
	0.23	8.757E-02	8.947E-01
	0.50	1.464E-01	1.930
	1.00	2.310E-01	3.800
	2.30	3.682E-01	8.533
	5.00	5.810E-01	1.795E+01
	10.00	7.695E-01	3.450E+01
16.0	0.05	7.707E-02	.1915
	0.10	1.164E-01	3.820E-01
	0.23	.2049	.8671
	0.50	.3306	1.855
	1.00	0.5035	3.630
	2.30	.8223	8.004
	5.00	1.214	1.65e1
	10.00	1.572	3.120E+01
18.0	0.05	.1245	.201
	0.10	.2062	.397
	0.23	.3536	.8924
	0.50	.585	1.885
	1.00	.8757	3.630
	2.30	1.434	7.797
	5.00	2.096	15.55
	10.00	2.649	28.4

H, km	V_∞, km/s / ρ_∞, kg/m^3	8.0	8.5	9.0	9.5	10.0	11.0	12.0	14.0	16.0	18.0
30	1.8410E-2	✔	✔	✔	✔	✔	✔	✔			
36	7.2579E-3	✔	✔	✔	✔	✔	✔	✔	✔		
42	2.9948E-3	✔	✔	✔	✔	✔	✔	✔	✔		
48	1.3167E-3			✔	✔	✔	✔	✔	✔	✔	
54	6.3137E-4			✔	✔	✔	✔	✔	✔	✔	✔
60	3.0592E-4			✔	✔	✔	✔	✔	✔	✔	✔
66	1.4713E-4			✔	✔	✔	✔	✔	✔	✔	✔
72	6.6593E-5			✔	✔	✔	✔	✔	✔	✔	✔
78	2.5239E-5			✔	✔	✔	✔	✔	✔	✔	✔
84	9.6940E-6			✔	✔	✔	✔	✔	✔	✔	✔

Figure 1. Flight Conditions Selected for Radiation Calculations.

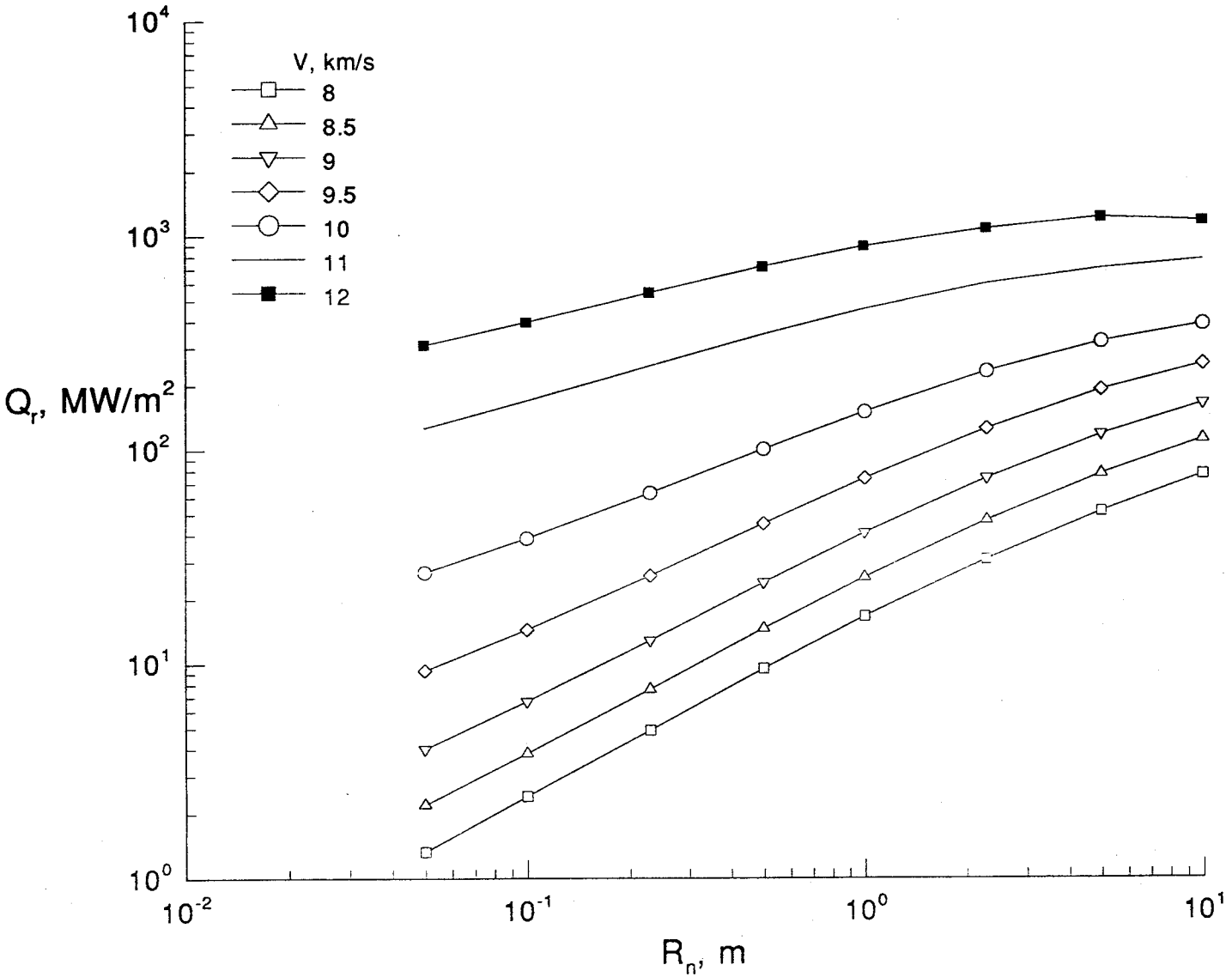

Figure 2. Radiative Heating Prediction at H=30 km. (ρ=1.8410E-2 kg/m^3)

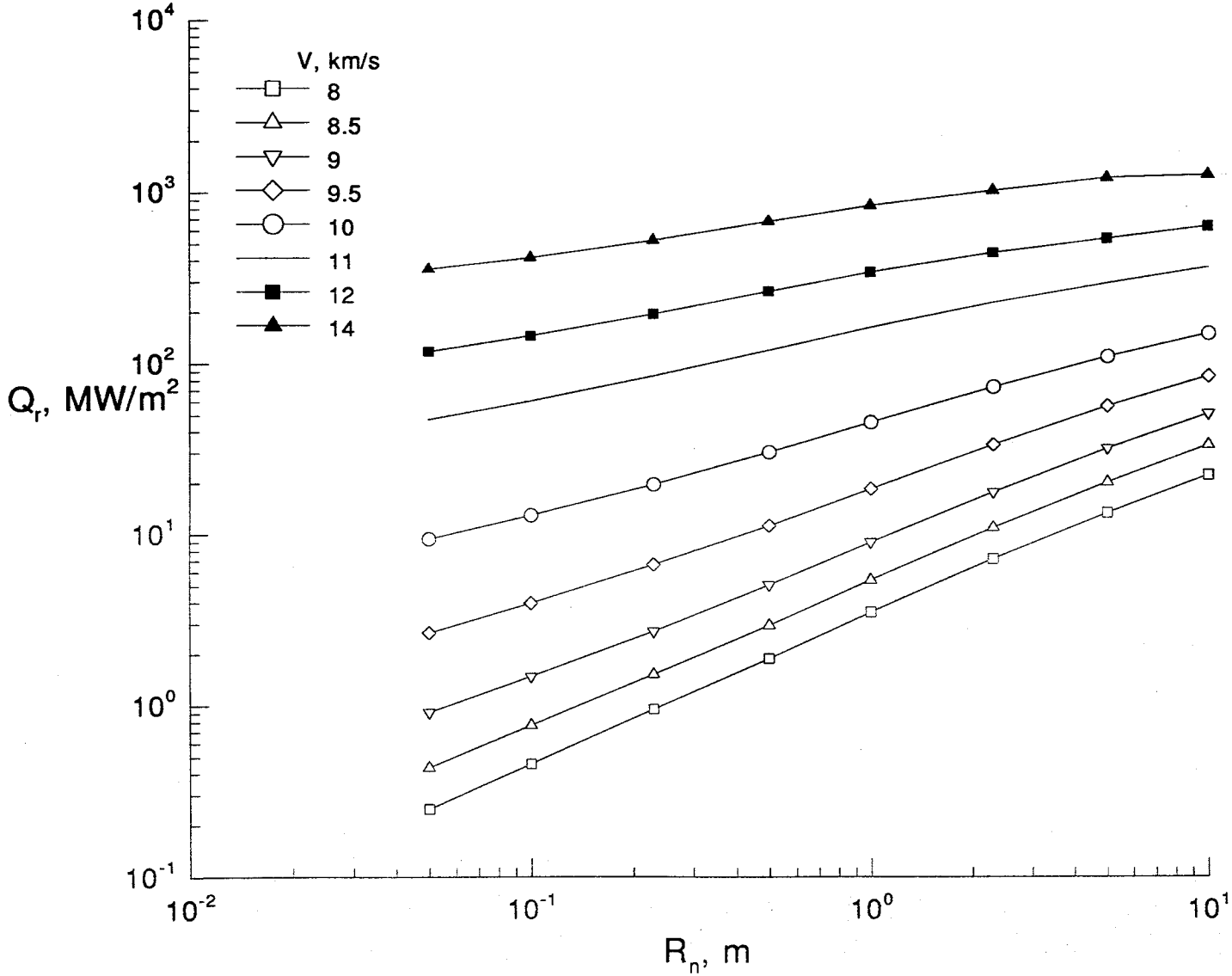

Figure 3. Radiative Heating Prediction at H=36 km. (ρ=7.2579E-3 kg/m^3)

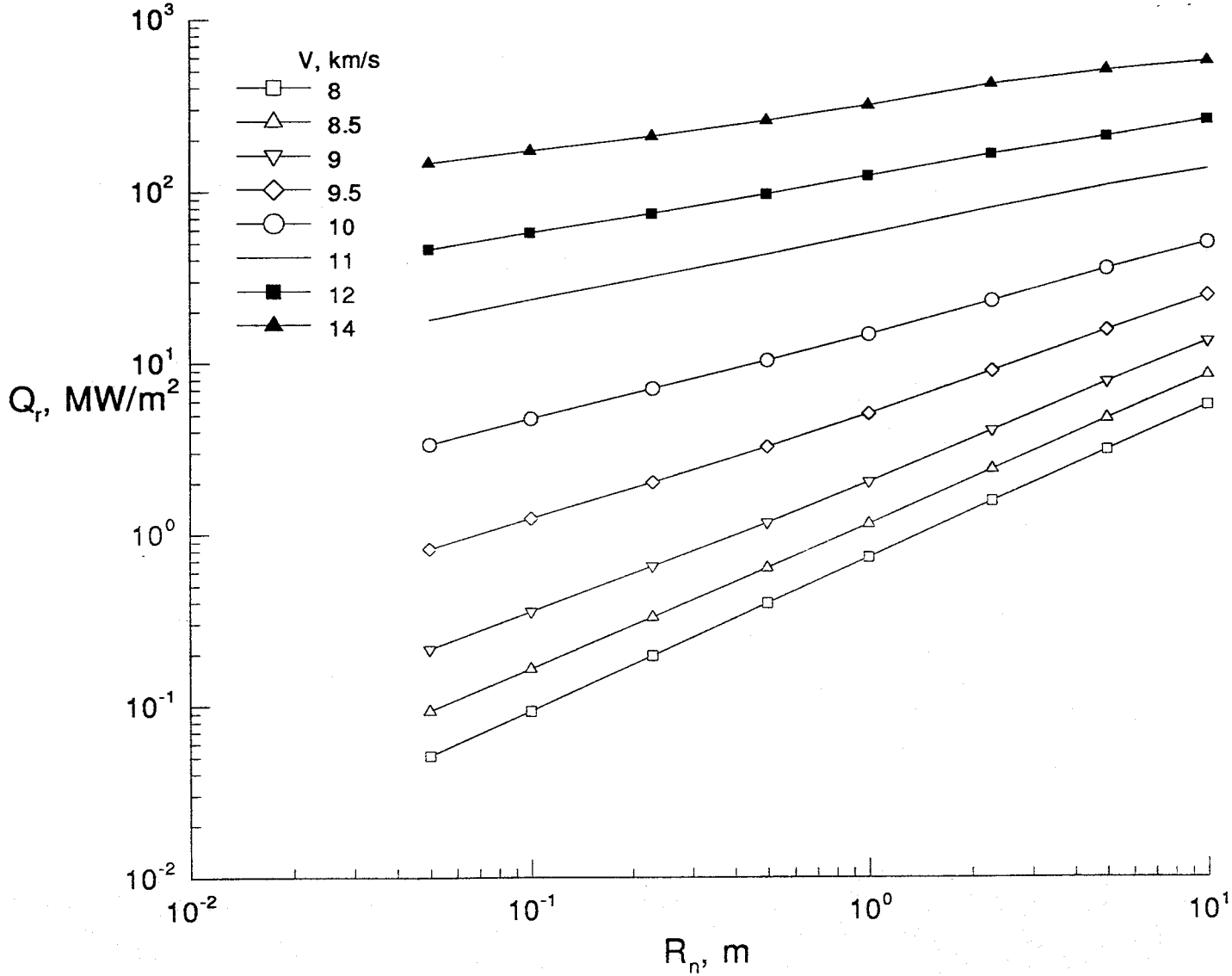

Figure 4. Radiative Heating Prediction at H=42 km. (ρ=2.9948E-3 kg/m^3)

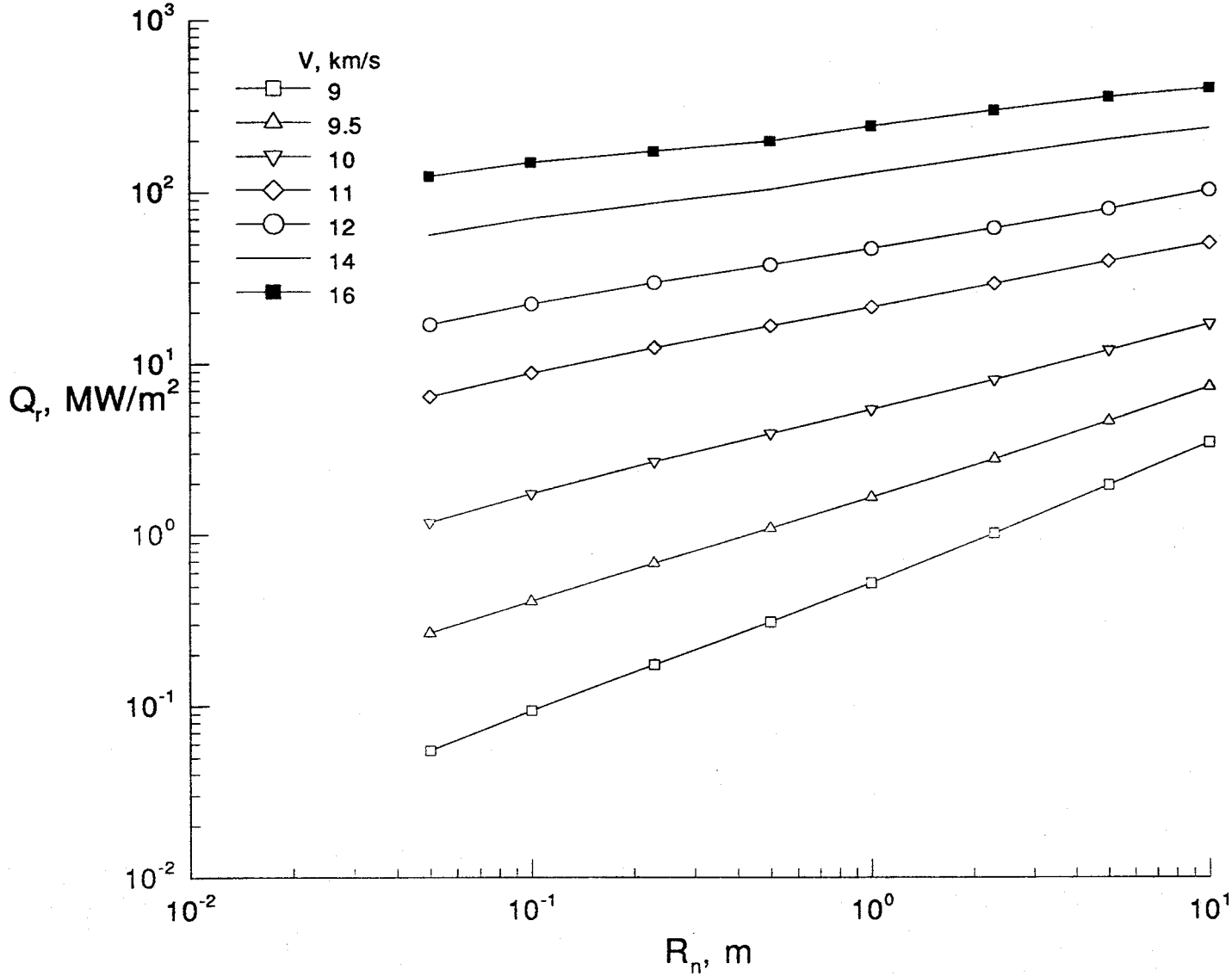

Figure 5. Radiative Heating Prediction at H=48 km. (ρ=1.3167E-3 kg/m^3)

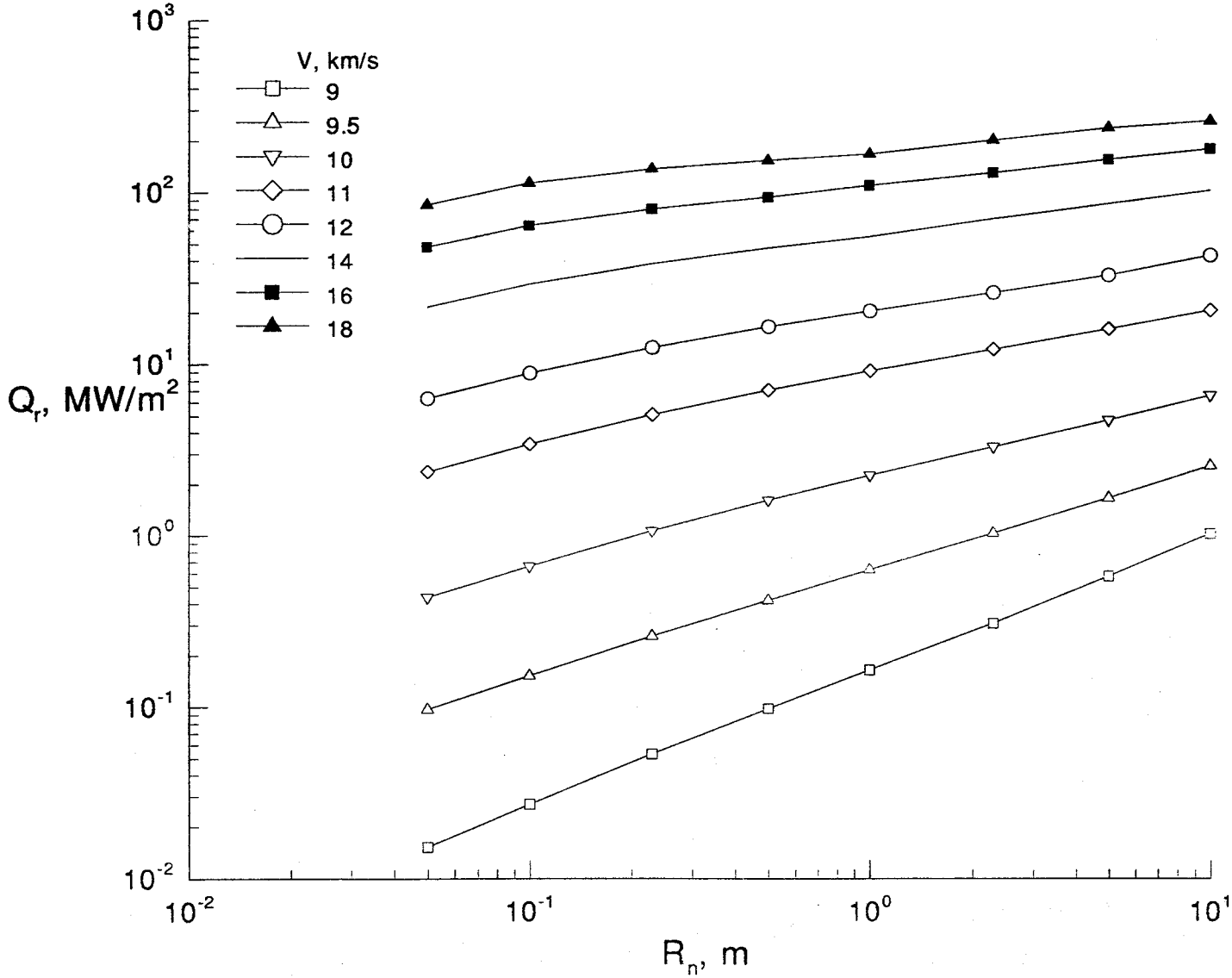

Figure 6. Radiative Heating Prediction at H=54 km. (ρ=6.3137E-4 kg/m^3)

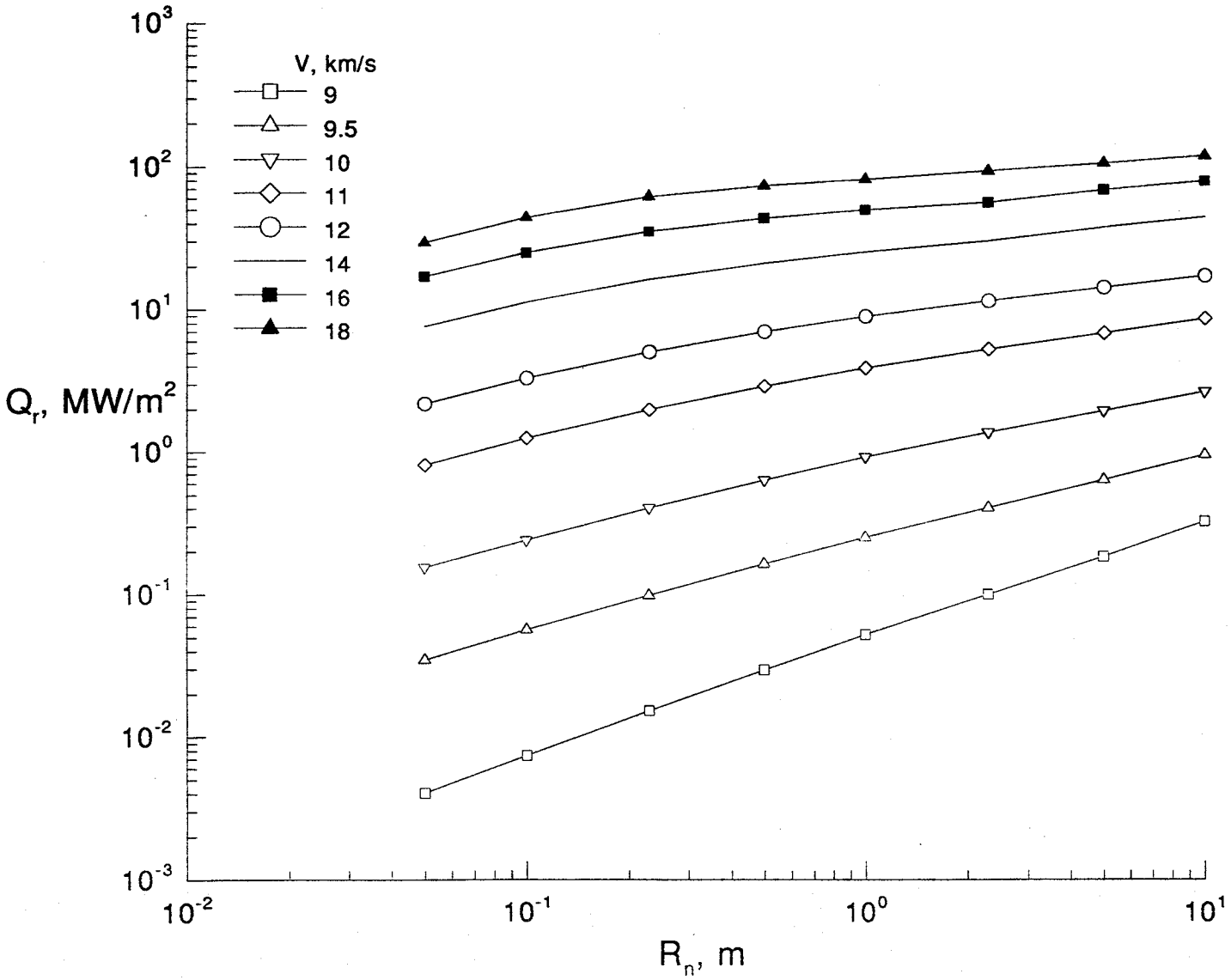

Figure 7. Radiative Heating Prediction at H=60 km. (ρ=3.0592E-4 kg/m^3)

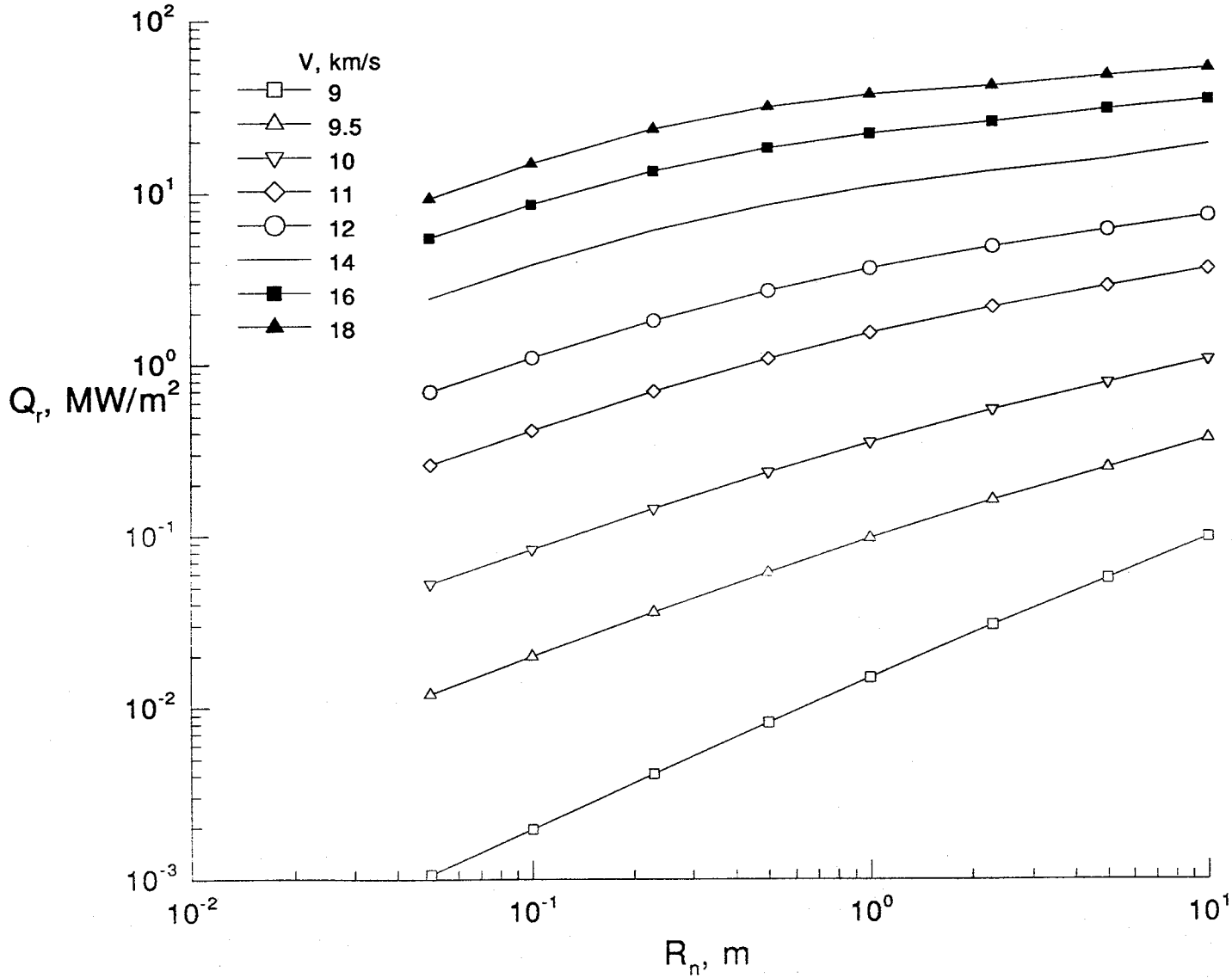

Figure 8. Radiative Heating Prediction at H=66 km. (ρ=1.4713E-4 kg/m^3)

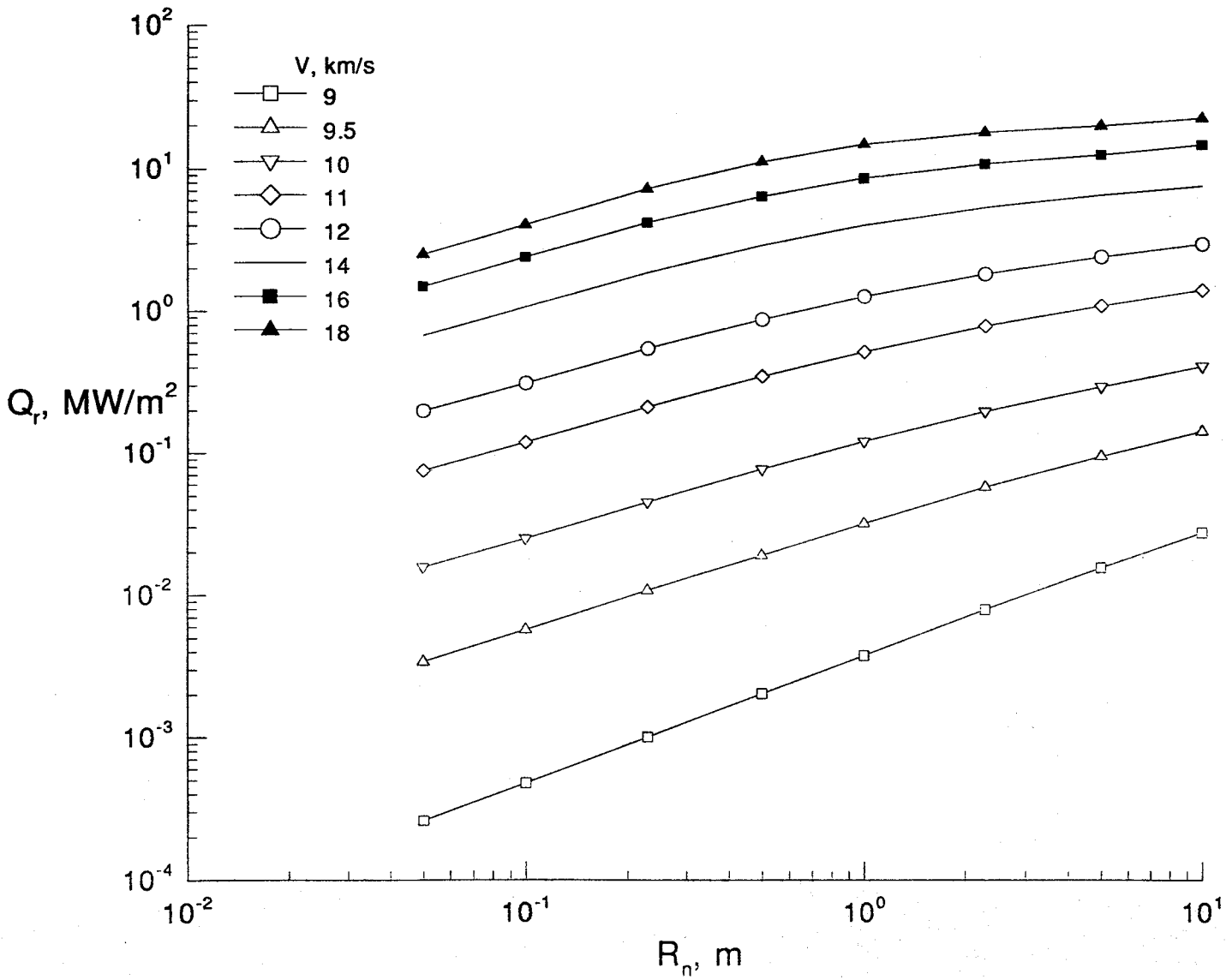

Figure 9. Radiative Heating Prediction at H=72 km. (ρ=6.6593E-5 kg/m^3)

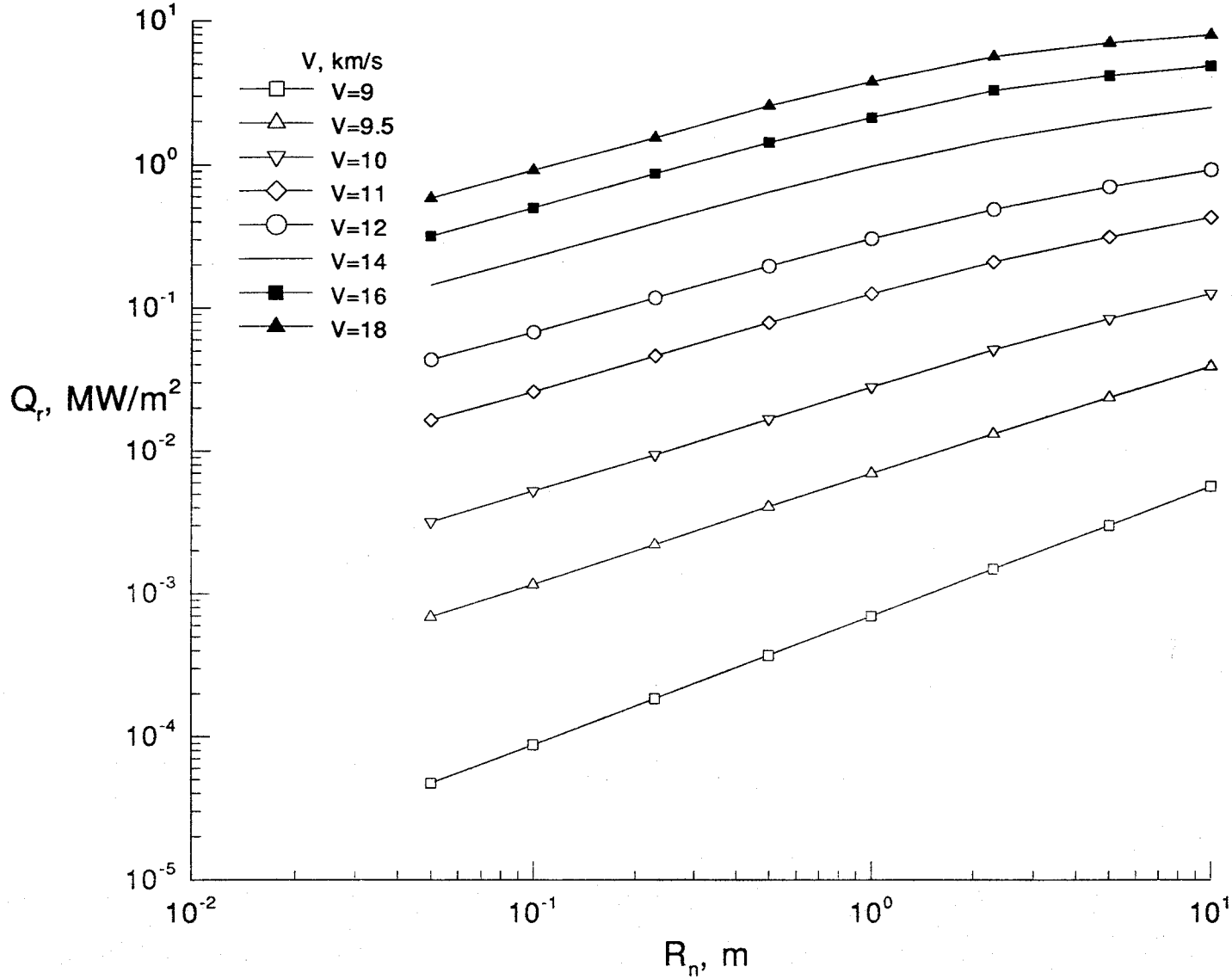

Figure 10. Radiative Heating Prediction at H=78 km. (ρ=2.5239E-5 kg/m^3)

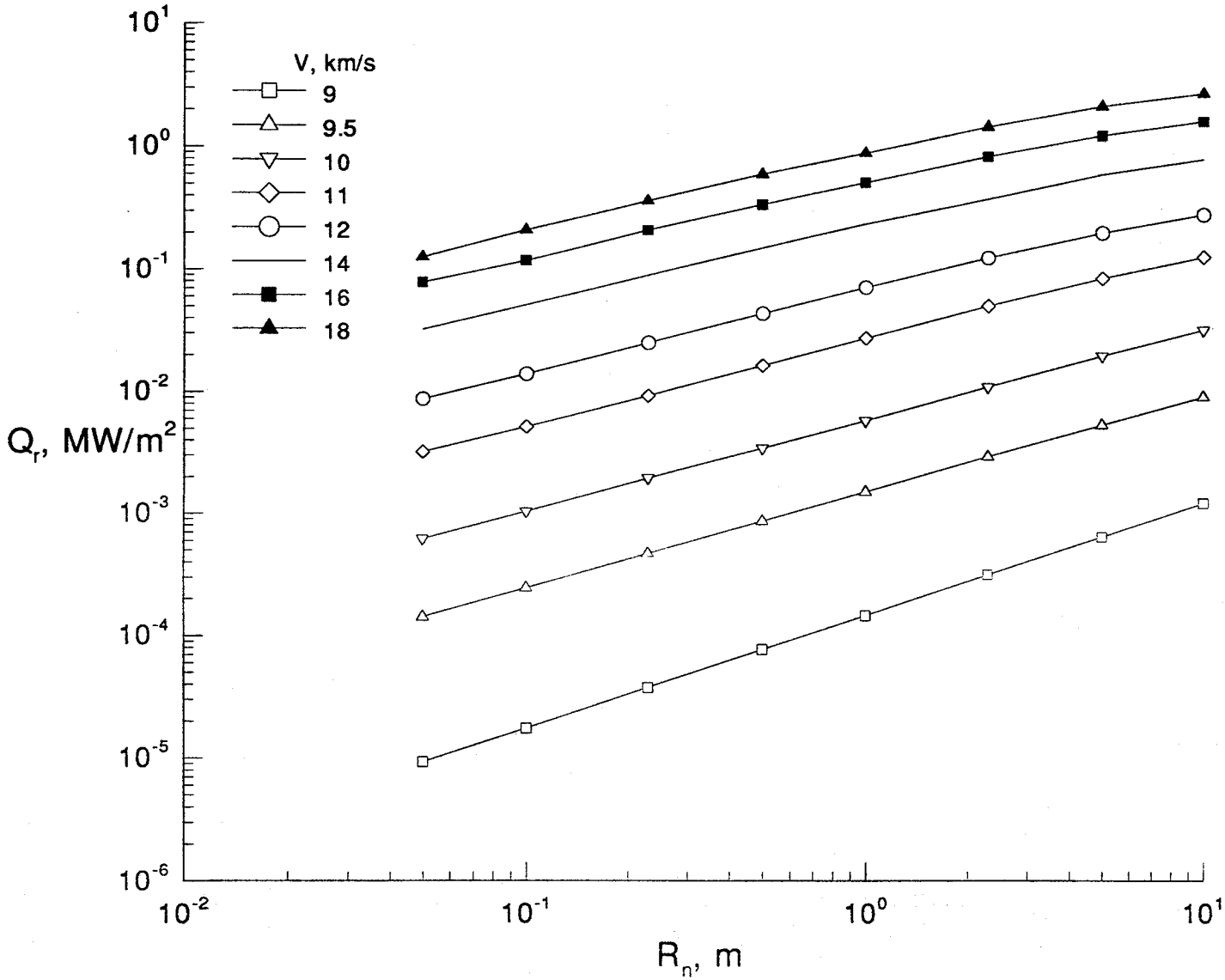

Figure 11. Radiative Heating Prediction at H=84 km. (ρ=9.6940E-6 kg/m^3)

NASA
National Aeronautics and Space Administration

Report Documentation Page

1. Report No.	2. Government Accession No.	3. Recipient's Catalog No.
NASA TM-102652		

4. Title and Subtitle	5. Report Date
Equilibrium Radiative Heating Tables for Earth Entry	May 1990
	6. Performing Organization Code

7. Author(s)	8. Performing Organization Report No.
Kenneth Sutton and Lin C. Hartung	
	10. Work Unit No. 506-40-91-01

9. Performing Organization Name and Address	11. Contract or Grant No.
NASA Langley Research Center Hampton, VA 23665-5225	
	13. Type of Report and Period Covered
12. Sponsoring Agency Name and Address	Technical Memorandum
National Aeronautics and Space Administration Washington, DC 20546-0001	14. Sponsoring Agency Code

15. Supplementary Notes

16. Abstract

The recent resurgence of interest in blunt-body atmospheric entry for applications such as aeroassisted orbital transfer and planetary return has engendered a corresponding revival of interest in radiative heating. Radiative heating may be of importance in these blunt-body flows because of the highly energetic shock layer around the blunt nose. Sutton developed an inviscid, stagnation point, radiation-coupled flow-field code for investigating blunt-body atmospheric entry. The method has been compared with ground-based and flight data, and reasonable agreement has been found. To provide information for entry body studies in support of lunar and Mars return scenarios of interest in the 1970's, the code was exercised over a matrix of Earth entry conditions. These results were never published. Recently, this matrix was extended slightly to reflect entry vehicle designs of current interest.

17. Key Words (Suggested by Author(s))	18. Distribution Statement
Radiative heating Equilibrium Aerobraking	Unclassified-Unlimited Subject Category 34

19. Security Classif. (of this report)	20. Security Classif. (of this page)	21. No. of pages	22. Price
Unclassified	Unclassified	26	A03